



Synthesis of high nitrogen doping of carbon nanotubes and modeling the stabilization of filled DAATO@CNTs (10,10) for nanoenergetic materials

Yu Zhong^a, Mounir Jaidann^b, Yong Zhang^a, Gaixia Zhang^a, Hao Liu^a, Mihnea Ioan Ionescu^a, Ruying Li^a, Xueliang Sun^{a,**}, Hakima Abou-Rachid^{b,*}, Louis-Simon Lussier^b

^a Department of Mechanical and Materials Engineering, The University of Western Ontario, London, Ontario, Canada, N6A 5B8

^b Defense Research & Development Canada–Valcartier, 2459 Boulevard Pie XI North, Quebec, Canada G3J 1X5

ARTICLE INFO

Article history:

Received 1 June 2009

Received in revised form

24 July 2009

Accepted 31 July 2009

Keywords:

A. Nanostructures

B. Vapour deposition

ABSTRACT

In this work, we have performed synthesis of nitrogen-doped carbon nanotubes using chemical vapor deposition method. Morphology, structure and composition of the carbon nanotubes (CNTs), as well as concentration and distribution of nitrogen inside CNTs are characterized by scanning electron microscopy, transmission electron microscopy, X-ray dispersive spectroscopy and X-ray photoelectron spectroscopy techniques. A bamboo-like structure of the nitrogen-doped CNTs has been observed. Temperature dependency on the synthesis of nitrogen-doped carbon nanotubes has been investigated and discussed. Diameter and growth rate of these hybrid materials are obviously temperature dependent. Nitrogen concentration inside the CNTs increases with declining synthesis temperature. Nitrogen-doped CNTs with nitrogen content up to 10.4 at% can be achieved at a low temperature of 800 °C. Synthesis of the high nitrogen CNTs proposes a feasible way to develop novel nanoenergetic materials. Besides the experimental study, we have carried out Density Functional Theory calculations on five energetic molecules named n-oxides of 3,3'-azo-bis(6-amino-1,2,4,5-tetrazine) (DAATO), where n = 1–5 refer to oxygen atoms, encapsulated in CNTs (10,10), in order to investigate the chemical stabilization of filled DAATO_n inside CNTs (10,10). In fact, the predicted adsorption energy values confirmed the chemical stability of the hybrid systems DAATO_n@CNTs (10,10) under normal conditions.

© 2009 Elsevier Ltd. All rights reserved.

1. Introduction

High energetic materials are characterized as a strong exothermic reactivity, which has made them much desirable for military and commercial applications. Most traditional high energetic materials such as rocket fuel and high explosives (TNT, RDX, and HMX) contain harmful substances and their combustion mainly produces ON_x production, creating significant environmental hazards. These high explosives derive most energy from oxidation of the carbon backbone, characterized as sensitivity to electrostatic discharge, friction, and impact. To deal with sensitivity and environment considerations, several approaches are being pursued to provide new energetic materials to meet the challenges of the future. Indeed, nanoenergetic materials have recently attracted great interest due to their novel interaction and functionality at the molecular level, which exhibit more promising performance than those of their bulk or micro-counterparts in

terms of the energy release rate, fuel consumption efficiency and materials homogeneity [1,2]. Among various nanoenergetic materials, nanostructured polymeric nitrogen possesses highest energy density. However, nanostructured polynitrogen chain is not mechanical and thermodynamic stable under ambient conditions [3–5]. Recently, we have found, using modeling, that an eight-atom nitrogen chain could be stable at ambient temperatures and pressures if it could be formed inside a carbon nanotube [6].

Since the discovery of carbon nanotube by Iijima in 1991 [7], carbon nanotubes has attracted much research interest due to the unique structure and potential applications [8–10]. Our interests are to dope nitrogen and increase its concentration inside carbon nanotubes and thereby provide more opportunities to form nitrogen-rich energetic nanostructures with high energy density, from theoretical and experimental point of views.

So far, various experimental methods have been utilized to produce nitrogen-doped carbon nanotubes, mainly divided into five types [11]: (1) chemical vapor deposition (CVD) [12]; (2) high-temperature and high-pressure reaction; (3) gas–solid reaction of amorphous carbon with NH₃ at high temperature [13]; (4) solid reaction [14] and; (5) solvothermal synthesis [15]. Thermal

** Also corresponding author.

* Corresponding author. Tel.: +1 418 844 4000x4048.

E-mail addresses: xsun@eng.uwo.ca (X. Sun),

Hakima.Abou-Rachid@drdc-rddc.gc.ca (H. Abou-Rachid).

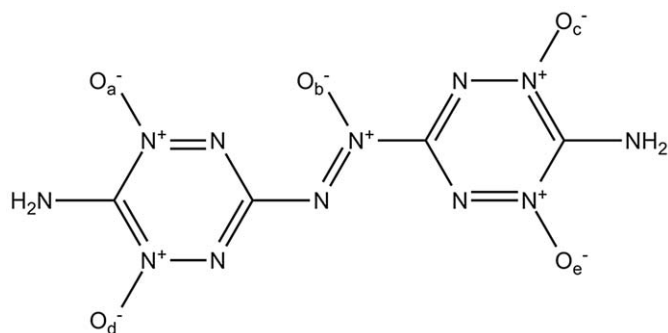


Fig. 1. Chemical structure of DAATO, where a, b, c, d and e are 0 or 1 and $a+b+c+d+e$ is from 1 to 5.

chemical vapor deposition method is one of the most facile approaches in which different nitrogen content can be incorporated in carbon nanotubes by using various precursors [11,16,17]. Melamine ($C_3N_6H_6$) is one economical source of C and N with low melt temperature around 360°C [18], which has similar atomic arrangement to that of C_3H_4 [19]. Catalytic decomposition of melamine can generate pre-existing C–N bonds, which may promote the formation of carbon nanotubes with high nitrogen concentration [11,20,21].

In this paper, we describe the synthesis of N-CNTs with CVD method by pyrolyzing melamine as the precursor in an atmospheric pressure. A thin Fe film is used as the catalyst. During the study, we found that the growth of N-doped CNTs is strongly dependent on the synthesis temperature. High nitrogen concentration up to 10.4 at% can be obtained within the N-doped CNTs at a temperature of 800°C . Morphology, structure, nitrogen concentration and distribution of N-doped CNTs have been analyzed.

The modeling work was carried out in order to investigate the chemical stability of nitrogen-rich compounds n-oxides of 3,3'-azo-bis(6-amino-1,2,4,5-tetrazine) (DAATO) (Fig. 1), where $n = 1\text{--}5$ refer to oxygen atoms in DAATO inside carbon nanotubes, using first-principles simulations in the framework of density functional theory in condensed phases.

2. Experimental

N-CNTs were prepared via CVD method by pyrolyzing melamine under an Ar atmosphere in a horizontal glass tube, where melamine was the only source of both carbon and nitrogen. A quartz boat containing melamine was loaded in the tube near the entrance of the furnace, which was mounted in the tube furnace, while a Si/SiO₂ wafer, which was pretreated by depositing Fe film (5 nm) on top, was placed in the center of the tube. Ar flow was introduced into the tube as gas carrier. After the furnace was heated up to the synthesis temperature ($800, 900$ and 980°C), the furnace was kept for 15 min and finally cooled down to room temperature. The products growing on the substrate were characterized by scanning electron microscopy (SEM), transmission electron microscopy (TEM) and X-ray photoelectron spectroscopy (XPS).

3. Computational details

Calculations were performed with the density functional theory (DFT) implemented in Dmol³ package [22,23]. All-electron spin unrestricted calculations are carried out with double numerical plus d-function basis set (DND), which provides reasonable accuracy for modest computational cost. We use the

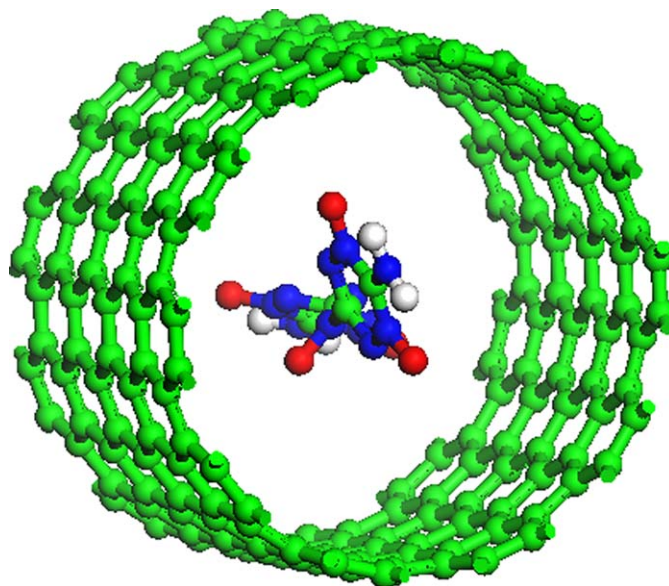


Fig. 2. The structural geometric of DAATO@CNT(10,10).

Perdew–Wang 91 (PW91) based on the generalized gradient approximation (GGA) of (DFT) [24].

The confinement of DAATO inside (10,10) carbon nanotube is treated as a triclinic cell size $17.58 \times 17.58 \times 12.90 \text{ \AA}^3$. All confined DAATO molecules inside CNT (Fig. 2), were optimized at DFT method.

Our simulations focused on the determination of adsorption energy of the DAATO molecules encapsulated in a (10,10) CNT. The adsorption energy of these molecules is defined as the energy difference between the total energy of the hybrid material (DAATO_n@CNT) and the energies of the isolated systems (DAATO_n and CNT). The adsorption energy observable value will provide us how these molecules may be stable inside CNT at the ambient conditions of temperature and pressure.

4. Results and discussion

4.1. Experimental results

Fig. 3 shows SEM and TEM images of N-CNTs grown at the temperature ranging from 800 to 900°C . SEM images (Fig. 3a, c and e) illustrate the general morphology of aligned N-CNTs grown on the Si wafer. It clearly shows that all the N-CNTs synthesized at $800, 900$ and 980°C have curly entangled structures. At a high temperature of 980°C , N-CNTs are $18 \mu\text{m}$ in length (Fig. 3a). When the temperature goes down to a lower temperature of 900°C , the length decreases to about $15 \mu\text{m}$ (Fig. 3c). Further decrease of the temperature down to 800°C , very short N-CNTs are obtained with $6 \mu\text{m}$ in length (Fig. 3e). If the temperature is too low, less than 800°C , the growth of N-CNTs is inhibited, while if the temperature is higher than 980°C , the morphology is quite similar to that of N-CNTs synthesized at 980°C . All the above results indicate the growth of N-CNTs is temperature dependent. The dependence of the CN_x growth rate on temperature can be related to several factors such as concentration, diffusion rate of the involved atoms and the growth rate at the interface between the catalyst and the formed nanotube. It is generally agreed that the diffusion of carbon is the key step determining the growth of carbon nanostructures [25]. With increasing temperature, diffusion rate of carbon and nitrogen atoms increases significantly, and the growth rate of the CN_x is significantly promoted.

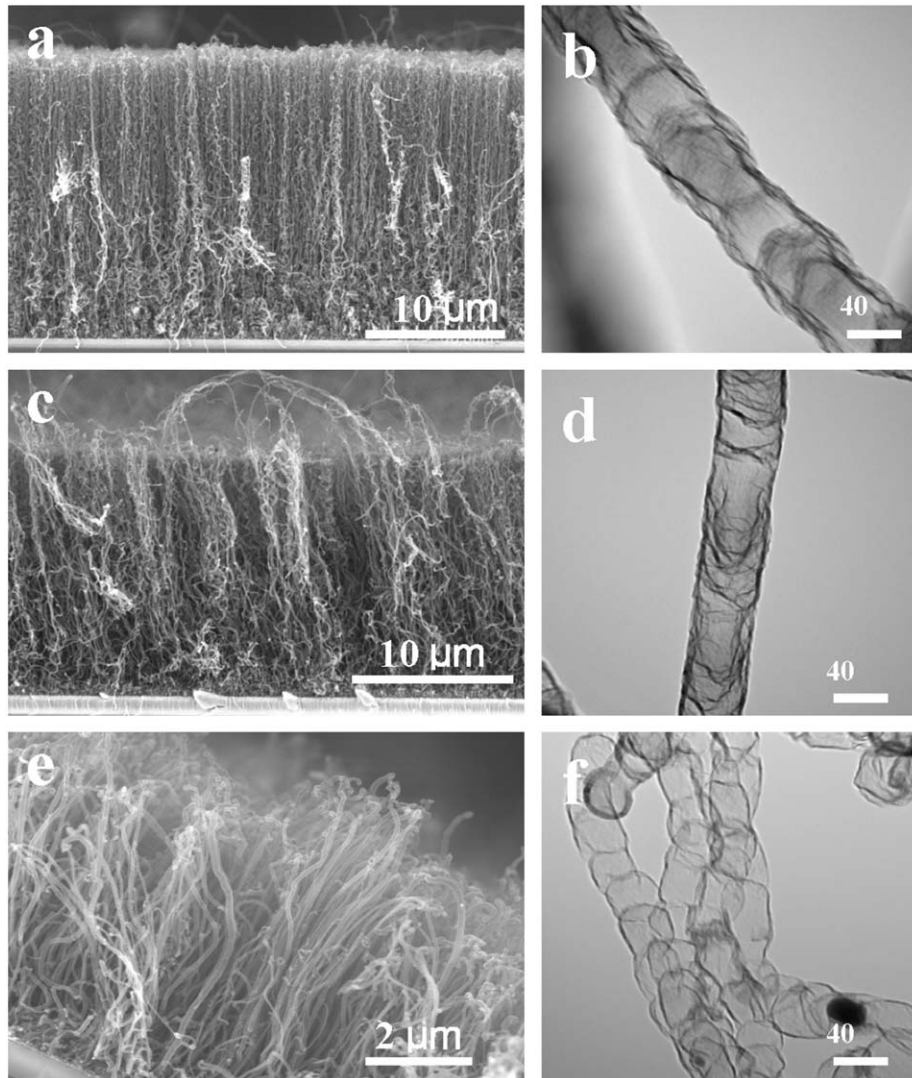


Fig. 3. SEM and TEM images of temperature-dependent growth of N-CNTs. (a) and (b) for the morphology of N-CNTs synthesized at 980 °C; (c) and (d) for the morphology of N-CNTs synthesized at 900 °C; (e) and (f) for the morphology of N-CNTs synthesized at 800 °C.

TEM images show the further information of the structure of N-CNTs. All the N-CNTs exhibit bamboo-like structure. The distribution of segments is periodical along the axis of the nanostructure. The diameter of N-CNTs varies with the temperature. At 980 °C, general observation indicates that the diameter of N-CNTs is between 40 and 85 nm. Fig. 2b shows a typical single N-CNTs with an average diameter of 75 nm. As the temperature goes down, the diameter also decreases. At 900 °C, the diameter is in a narrow range from 40 to 60 nm. Fig. 3d shows a TEM image of single N-CNT with the diameter of 60 nm. At 800 °C, the diameter of N-CNTs is only around 30 nm (Fig. 3f). As the growth temperature decreases, less agglomeration of the catalyst occurs, resulting in smaller sized catalysts and thinner N-CNTs.

The synthesis temperature can also affect the morphology of the compartment layers. At the high temperature (980 °C), the graphitic layers are flat, while at the low temperature (800 °C), the layers become corrugated as shown in HRTEM Fig. 4. The results indicate that the lower synthesis temperature usually results in the curled and disordered graphitic layers; while the higher temperature favors the formation of a well-graphitic structure [26].

It should be noted that the investigation on C–N bonding is an essential issue to explore the potential of CN_x as a nanoenergetic

material and/or host. It has been reported that nitrogen doping with carbon nanotubes can create well localized and highly chemically active sites on the carbon surface [27]. When carbon nanotubes are filled with high-density energetic materials, e.g. a polymeric nitrogen chain, an effective electric field will be created between the active carbon nanotube surface and the nitrogen chain where the C–N distance is minimal. This will stabilize the high energetic chain that is unstable at ambient conditions [6], which favors the control and utilization of high energetic materials. To measure the N content and study the C–N bonding in the nanotubes, XPS study was carried out after the synthesis. Fig. 5a shows a survey scan spectrum of the N-CNTs prepared at 800 °C. The peaks of C 1s, N 1s and O 1s are labeled at 285, 401 and 531 eV, respectively. The oxygen signal might originate from oxygen functional groups and/or the residual air in the nanotubes.

Two samples synthesized at 980 and 800 °C were characterized by XPS, with the nitrogen contents of 1.7 and 10.4 at%, respectively. The result indicates the lower synthesis temperature leads to the higher nitrogen content within the nanotubes. At lower temperatures, the decomposition source of melamine is mainly composed of the pyrolysis radicals containing a C–N bond, which is a key factor to obtain high nitrogen concentration of CN_x . Therefore, lower temperatures favor the growth of CN_x with

higher nitrogen contents, which is similar to the previous report using dimethylformamide as the pyrolysis precursor [26]. Fig. 5b and c show the high-resolution N 1s XPS spectra of as-grown CNTs synthesized at 980 and 800 °C, respectively. The N 1s peak can be

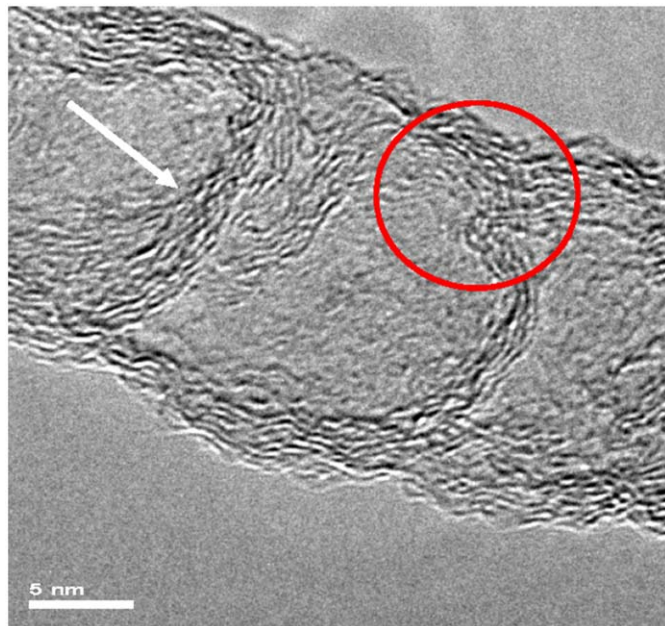


Fig. 4. HRTEM image of N-doped CNTs synthesized at 800 °C. Arrow points the interlinks inside a nanotube; disordered layers are labeled with circle.

deconvoluted into five main component peaks, representing pyridinic nitrogen (N_P at 398 eV), pyrrolic nitrogen (N_{PYR} at 399 eV), quaternary nitrogen (N_Q at 401 eV) and nitrogen oxides (N_{OX1} at 404 eV and N_{OX2} at 406 eV) [28–30]. In pyridinic nitrogen structure, the N atom is sp^2 hybridized bonding with two C atoms, while in the quaternary nitrogen structure, a C atom is substituted by a N atom in the graphitic sheet [30]. The pyrrolic nitrogen is sp^3 hybridized in a five-member ring [28].

The synthesis temperature can affect the type of nitrogen configuration in the graphitic layers. For the N-doped CNTs synthesized at 980 °C, the area composition of N_P , N_{PYR} , N_Q , N_{OX1} and N_{OX2} is 19.2%, 7.6%, 60.7%, 8.2% and 4.3%, respectively. The relative intensity of N_P/N_Q is 0.32, indicating that the nitrogen atoms incorporated into the CNTs are mainly in the form of quaternary nitrogen. When the temperature goes down to 800 °C, the feature of XPS spectrum is similar to that of N-doped CNTs synthesized at 980 °C, except the obvious percentage change in the area composition of N_P and N_Q . The area composition of N_P , N_{PYR} , N_Q , N_{OX1} and N_{OX2} is 54.6%, 3.1%, 30.2%, 7.2% and 4.9%, respectively. As temperature decreases, the percentage of N_Q in total amount of N decreases, in contrast, the percentage of N_P becomes much greater. The relative intensity of N_P/N_Q increases to 1.81. The change in the relative intensity indicates that the atomic ratio of pyridinic nitrogen in total nitrogen atoms increases as the temperature decreases. Compared with quaternary nitrogen, pyridinic nitrogen has a lower thermal stability [31]. That is, the higher synthesis temperature would favor the formation of quaternary nitrogen in the graphitic layers, while the lower synthesis temperature will lead to the more incorporation of nitrogen in term of pyridinic nitrogen.

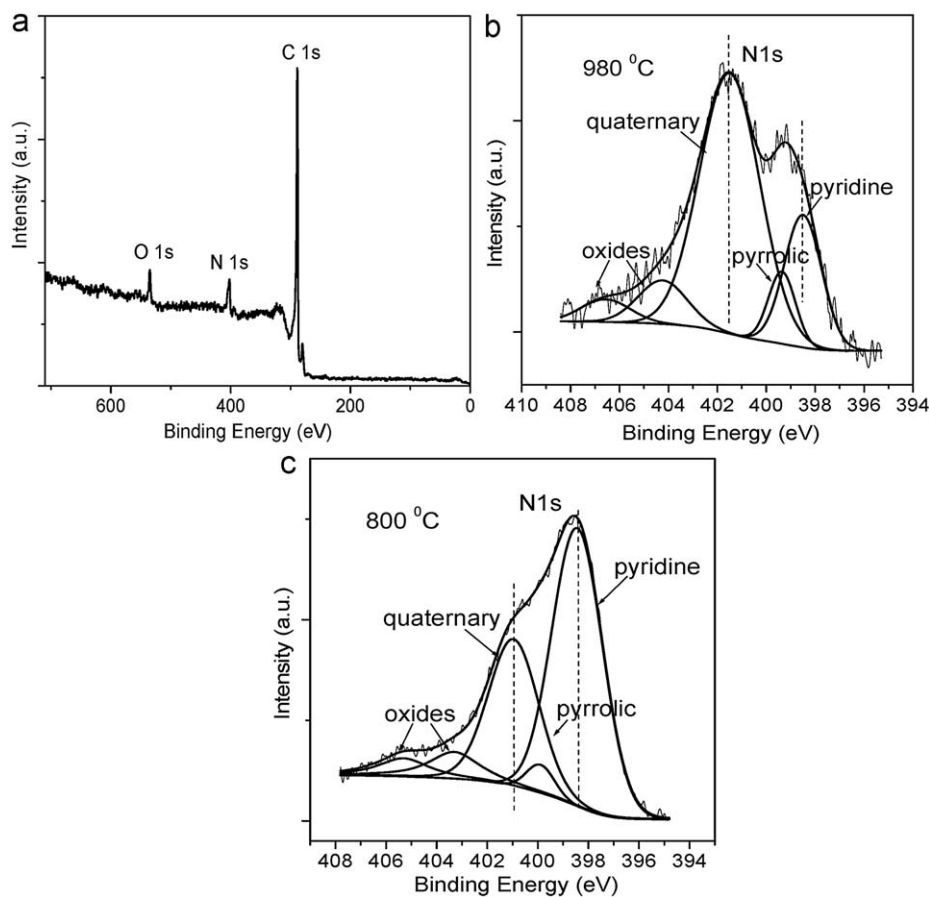


Fig. 5. XPS spectra of the N-doped CNTs. (a) A survey scan of the N-doped CNTs synthesized at 800 °C, (b) and (c) N 1s XPS spectra of N-doped CNTs synthesized at 980 and 800 °C, respectively.

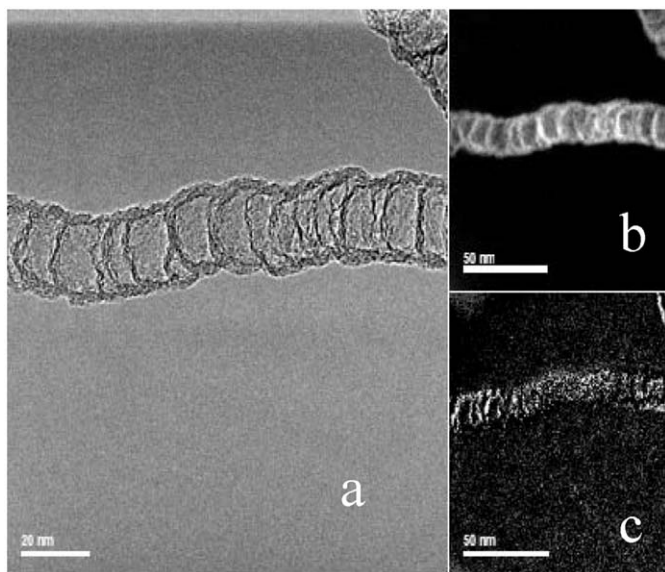


Fig. 6. Mapping images of N-doped CNTs synthesized at 800 °C. (a) TEM image of N-doped CNT; (b) and (c) C and N distribution in N-doped CNT, respectively.

In addition, combining the XPS analysis and the TEM images, it is obvious that the increase in pyridinic nitrogen results in the defects in the graphite layers [32], like disorder interlinks clearly shown in HRTEM images (Fig. 4). The TEM images (shown in Figs. 3 and 4) also show the tendency of changing in the diameters, i.e. thinner nanotubes are more readily obtained at lower temperature. Compared with quaternary nitrogen, pyridinic nitrogen is more favorable in as-grown CNTs with small diameter [32]. Then the percentage of pyridinic nitrogen is considered to increase in the total amount of N in the nanotubes, which consists with XPS results.

According to the mapping results (Fig. 6), the distribution of C atoms along the axis of nanotube is uniform, while N atoms usually concentrate at the disordered layers and interlinks resulting from the incorporation of N during the growth process.

4.2. Modeling results

We have chosen to use a (10,10) carbon nanotube as a nanoscale matrix to host DAATO molecules. It was mentioned in the literature that the DAATO contains an average of 3.2–3.6 oxygen atoms per molecule [33], which gives five possibilities for positioning and quantifying oxygen atoms per molecule (Fig. 1). The symbol DAATO_n refers to molecules DAATO with $n = 1-5$ oxygen atoms in the molecule.

Table 1 shows the predicted adsorption energies of the five molecules studied. From this table we note that all adsorption energy values are negative. Therefore, the chemical stability of the hybrid materials DAATO_n@CNT (10,10) is confirmed. However, the lowest adsorption energy of the hybrid material is provided by the DAATO molecule involving two oxygen atoms inside CNT (10,10) (−1.19 eV). This conclusion is explained again in terms of higher electronic charge transfer from CNT to the DAATO_2 molecule inside CNT (10,10) compared with the other DAATO_n molecules. In other words, this charge transfer is the result of Van der Waals and electrostatic interactions that occur between CNT and DAATO_n molecules.

5. Conclusions

N-doped CNTs with high nitrogen concentration (up to 10.4 at%) have been obtained by pyrolyzing melamine under an

Table 1

Adsorption energies (E_{ad}) in eV of DAATO_n@CNT (10,10) hybrid materials.

Hybrid materials	E_{ad}^a
DAATO_1@CNT(10,10)	−0.31
DAATO_2@CNT(10,10)	−1.19
DAATO_3@CNT(10,10)	−0.41
DAATO_4@CNT(10,10)	−0.37
DAATO_5@CNT(10,10)	−0.68

^a 1 eV = 1602 × 10^{−19} J

atmosphere pressure. Synthesis temperature ranges from 800 to 980 °C. The growth of N-doped CNTs is temperature dependent, i.e. the diameter and length decrease as the temperature goes down, while more defects are introduced in terms of disorder graphitic layers and interlinks inside the tubes. Due to the incorporation of nitrogen into CNTs, bamboo-like structure is induced, and nitrogen mainly concentrates at disordered layers and inner interlinks. The XPS analysis demonstrates that the lower synthesis temperature leads to the higher N content, especially much higher content of pyridinic N component, in N-CNTs. Therefore, realization of high nitrogen doping within CNTs will inevitably provide more opportunities to develop nitrogen-rich energetic nanostructures with high energy density.

Molecular modeling studies of DAATO_n@CNT show, through the calculations of the adsorption energies, that all hybrid materials DAATO_n@CNT(10,10) are chemically stable at ambient conditions. Further modeling work is progress on the assessment of the high performance of these hybrid materials by calculating heats of formation of these hybrid materials.

Acknowledgements

This research was supported by Department of National Defence (DND) and National Science and Engineering Council of Canada (NSERCC).

References

- [1] C. Rossi, K.L. Zhang, D. Estève, P. Alphonse, P. Tailhades, C. Vahlas, Nanoenergetic materials for MEMS: A review, *J. Microelectromech. Syst.* 16 (2007) 919–931.
- [2] K.L. Zhang, C. Rossi, G.A. Ardila Rodriguez, C. Tenailleau, P. Alphonse, Development of a nano-Al/CuO based energetic material on silicon substrate, *Appl. Phys. Lett.* 91 (2007) 113117–113119.
- [3] M.I. Eremets, R.J. Hemley, H.-K. Mao, E. Gregoryanz, Semiconducting non-molecular nitrogen up to 240 GPa and its low-pressure stability, *Nature* 411 (2001) 170–174.
- [4] K.O. Christie, Recent advances in the chemistry of N₅⁺, N₅[−] and high-oxygen compounds, *Propellants, Explos., Pyrotech.* 32 (2007) 194–204.
- [5] M.I. Eremets, A.G. Gavriluk, I.A. Trojan, D.A. Dzivenko, R. Boehler, Single-bonded cubic form of nitrogen, *Nat. Mater.* 3 (2004) 558–563.
- [6] H. Abou-Rachid, A. Hu, V. Timoshevskii, Y. Song, L.-S. Lussier, Nanoscale high energetic materials: A polymeric nitrogen chain N₈ confined inside a carbon nanotube, *Phys. Rev. Lett.* 100 (2008) 196401.
- [7] S. Iijima, Helical microtubules of graphitic carbon, *Nature* 354 (1991) 56–58.
- [8] C. Liu, Y.Y. Fan, M. Liu, H.T. Cong, H.M. Cheng, M.S. Dresselhaus, Hydrogen storage in single-walled carbon nanotubes at room temperature, *Science* 286 (1999) 1127–1129.
- [9] J. Kong, N.R. Franklin, C.W. Zhou, M.G. Chapline, S. Peng, K. Cho, H.J. Dai, Nanotube molecular wires as chemical sensors, *Science* 287 (2000) 622–625.
- [10] P. Kim, C.M. Lieber, *Science* 286 (1999) 2148–2150.
- [11] X.C. Wu, Y.R. Tao, Y.N. Lu, L. Dong, Z. Hu, High-pressure pyrolysis of melamine route to nitrogen-doped conical hollow and bamboo-like carbon nanotubes, *Diamond Relat. Mater.* 15 (2006) 164–170.
- [12] J. Kouvetakis, M. Todd, B. Wilkens, A. Bandari, N. Cave, Novel synthetic routes to carbon–nitrogen thin films, *Chem. Mater.* 6 (1994) 811–814.
- [13] L.-W. Yin, Y. Bando, M.-S. Li, Y.-X. Liu, Y.-X. Qi, Unique single-crystalline beta carbon nitride nanorods, *Adv. Mater.* 15 (2003) 1840–1844.
- [14] T. Oku, M. Kawaguchi, Microstructure analysis of CN-based nanocage materials by high-resolution electron microscopy, *Diamond Relat. Mater.* 9 (2000) 906–910.

- [15] Q.X. Guo, Y. Xie, X.J. Wang, S.Y. Zhang, T. Hou, S.C. Lv, Synthesis of carbon nitride nanotubes with the C_3N_4 stoichiometry via a benzene-thermal process at low temperatures, *Chem. Commun.* 1 (2004) 26–27.
- [16] X.Y. Tao, X.B. Zhang, F.Y. Sun, J.P. Cheng, F. Liu, Z.Q. Luo, Large-scale CVD synthesis of nitrogen-doped multi-walled carbon nanotubes with controllable nitrogen content on a $Co_xMg_{1-x}MoO_4$ catalyst, *Diamond Relat. Mater.* 16 (2007) 425–430.
- [17] Y. Chai, Q.F. Zhang, J.L. Wu, A simple way to CN_x /carbon nanotube intramolecular junctions and branches, *Carbon* 44 (2006) 687–691.
- [18] John A. Dean, *Lange's Handbook of Chemistry*, 12th ed., McGraw-Hill Book Company, 1979.
- [19] I. Alves, G. Demazeau, B. Tanguy, F. Weill, On a new model of the graphitic form C_3N_4 , *Solid State Commun.* 109 (1999) 697–701.
- [20] J. Li, C.B. Cao, H.S. Zhu, Synthesis and characterization of graphite-like carbon nitride nanobelts and nanotubes, *Nanotechnology* 18 (2007) 115605.
- [21] S. Trasobares, O. Stéphan, C. Colliex, W.K. Hsu, H.W. Kroto, D.R.M. Walton, Compartmentalized CN_x nanotubes: chemistry, morphology, and growth, *J. Chem. Phys.* 116 (2002) 8966–8972.
- [22] B. Delley, An all-electron numerical method for solving the local density functional for polyatomic molecules, *J. Chem. Phys.* 92 (1) (1990) 508–517.
- [23] B. Delley, From molecules to solids with the DMol³ approach, *J. Chem. Phys.* 113 (18) (2000) 7756–7764.
- [24] J.P. Perdew, Y. Wang, Accurate and simple analytic representation of the electron–gas correlation energy, *Phys. Rev. B* 45 (23) (1992) 13244–13249.
- [25] Y.T. Lee, J. Park, Y.S. Choi, H. Ryu, H.J. Lee, Temperature-dependent growth of vertically aligned carbon nanotubes in the range 800–1100 °C, *J. Phys. Chem. B* 106 (2002) 7614–7618.
- [26] C.C. Tang, Y. Bando, D. Golberg, F.F. Xu, Structure and nitrogen incorporation of carbon nanotubes synthesized by catalytic pyrolysis of dimethylformamide, *Carbon* 42 (2004) 2625–2633.
- [27] K. Jiang, A. Eitan, L.S. Schadler, P.M. Ajayan, R.W. Siegel, N. Grobert, M. Mayne, M. Reyes-Reyes, H. Terrones, M. Terrones, Selective attachment of gold nanoparticles to nitrogen-doped carbon nanotubes, *Nano Lett.* 3 (2003) 275–277.
- [28] S. van Dommele, A. Romero-Izquierdo, R. Brydson, K.P. de Jong, J.H. Bitter, Tuning nitrogen functionalities in catalytically growth nitrogen-containing carbon nanotubes, *Carbon* 1 (2008) 138–148.
- [29] H. Chen, Y. Yang, Z. Hu, K.F. Huo, Y.W. Ma, Y. Chen, X.S. Wang, Y.N. Lu, Synergism of CN six-membered ring and vapour–liquid–solid growth of CN nanotubes with pyridine precursor, *J. Phys. Chem. B* 110 (2006) 16422–16427.
- [30] D.H. Lee, W.J. Lee, S.O. Kim, Highly efficient vertical growth of wall-number-selected N-doped carbon nanotube arrays, *Nano Lett.* 9 (2009) 1427–1432.
- [31] H.C. Choi, S.Y. Bae, W.-S. Jang, J. Park, H.J. Song, H.-J. Shin, H. Jung, J.-P. Ahn, Release of N from the carbon nanotubes via high-temperature annealing, *J. Phys. Chem. B* 109 (2005) 1683–1688.
- [32] S.H. Yang, W.H. Shin, J.K. Kang, The nature of graphite- and pyridinelike nitrogen configurations in carbon nitride nanotubes: dependence on diameter and helicity, *Small* 4 (2008) 437–441.
- [33] M.A. Hiskey, D.E. Chavez and D. Naud, Preparation of 3,3'-azobis(6-amino-1,2,4,5-tetrazine), US Patent 6342589, 2002, United States Department of Energy, USA.